











Dedicated 3D-T2-STIR-ZOOMit Imaging Improves Demyelinating Lesion Detection in the Anterior Visual Pathways of Patients with Multiple Sclerosis

 E. Pravata,  L. Roccatagliata,  M.P. Sormani,  L. Carmisciano,  C. Lienerth,  R. Sacco,  A. Kaelin-Lang,  A. Cianfoni,  C. Zecca, and  C. Gobbi



ABSTRACT

BACKGROUND AND PURPOSE: Demyelinating lesions in the anterior visual pathways represent an underestimated marker of disease dissemination in patients with MS. We prospectively investigated whether a dedicated high-resolution MR imaging technique, the 3D-T2-STIR-ZOOMit, improves demyelinating lesion detection compared with the current clinical standard sequence, the 2D-T2-STIR.

MATERIALS AND METHODS: 3T MR imaging of the anterior visual pathways (optic nerves, chiasm, and tracts) was performed using 3D-T2-STIR-ZOOMit and 2D-T2-STIR, in patients with MS and healthy controls. Two experienced neuroradiologists assessed, independently, demyelinating lesions using both sequences separately. 3D-T2-STIR-ZOOMit scan-rescan reproducibility was tested in 12 patients. The Cohen κ was used for interrater agreement, and the intraclass correlation coefficient for reproducibility. Between-sequence detection differences and the effects of location and previous acute optic neuritis were assessed using a binomial mixed-effects model.

RESULTS: Forty-eight patients with MS with ($n = 19$) or without ($n = 29$) past optic neuritis and 19 healthy controls were evaluated. Readers' agreement was strong (3D-T2-STIR-ZOOMit: 0.85; 2D-T2-STIR: 0.90). The 3D-T2-STIR-ZOOMit scan-rescan intraclass correlation coefficient was 0.97 (95% CI, 0.96–0.98; $P < .001$), indicating excellent reproducibility. Overall, 3D-T2-STIR-ZOOMit detected more than twice the demyelinating lesions ($n = 89$) than 2D-T2-STIR ($n = 43$) (OR = 2.7; 95% CI, 1.7–4.1; $P < .001$). In the intracranial anterior visual pathway segments, 33 of the 36 demyelinating lesions (91.7%) detected by 3D-T2-STIR-ZOOMit were not disclosed by 2D-T2-STIR. 3D-T2-STIR-ZOOMit increased detection of demyelinating lesion probability by 1.8-fold in patients with past optic neuritis (OR = 1.8; 95% CI, 1.2–3.1; $P = .01$) and 5.9-fold in patients without past optic neuritis (OR = 5.9; 95% CI, 2.5–13.8; $P < .001$). No false-positive demyelinating lesions were detected in healthy controls.

CONCLUSIONS: Dedicated 3D-T2-STIR-ZOOMit images improved substantially the detection of MS disease dissemination in the anterior visual pathways, particularly in the intracranial segments and in patients without past optic neuritis.

ABBREVIATIONS: AON = acute optic neuritis; aVP = anterior visual pathway; DL = demyelinating lesion; HC = healthy controls; iCanal = intracanalicular optic nerve; iCran = intracranial optic nerve; iOrb = intraorbital optic nerve; OC = optic chiasm; OT = optic tract; pON = past optic neuritis

MS is the most common immune-mediated demyelinating disease in young adults,¹ with frequent involvement of the visual pathways.² Pathologic investigations demonstrated a high prevalence of demyelinating lesions (DLs) in the anterior visual pathways (aVPs), including the optic nerve, chiasm (OC), and tract (OT), in patients either with or without previous episodes of

acute optic neuritis (AON).³ Accordingly, ophthalmologic studies showed frequent occurrence of subclinical visual impairment in MS, even in patients without previous AON.⁴ Nevertheless and despite a previous proposal,⁵ the aVPs are currently not included among the sites investigated by MR imaging to demonstrate disease dissemination in space, due to the lack of supportive data

Received July 15, 2020; accepted after revision December 20.

From the Departments of Neuroradiology (E.P., A.C.) and Neurology (R.S., A.K.-L., C.Z., C.G.), Neurocenter of Southern Switzerland, Lugano, Switzerland; Department of Health Sciences (L.R., M.P.S., L.C.), University of Genova, Genova, Italy; Dipartimento di Scienze della Salute – DISSAL (L.R., M.P.S.), Istituto di Ricovero e Cura a Carattere Scientifico Ospedale Policlinico San Martino, Genoa, Italy; Bayer Vital GmbH (C.L.), Leverkusen, Germany; and Faculty of Biomedical Sciences (A.K.-L., A.C., C.Z., C.G.), Università della Svizzera Italiana, Lugano, Switzerland.

C. Zecca and C. Gobbi contributed equally to this work.

E.P. and R.S. received funding from the Advisory Board for Research of the Hospital Cooperation (Ente Ospedaliero Cantonale) and from the Swiss Society of Multiple Sclerosis for conducting this study (grant No. EOC.NEURORAD.1701).

Please address correspondence to Emanuele Pravata, MD, Neurocenter of Southern Switzerland, Department of Neuroradiology, Via Tesserete 46, 6903, Lugano, Switzerland; e-mail: emanuele.pravata@eoc.ch

 Indicates article with online supplemental data.

<http://dx.doi.org/10.3174/ajnr.A7082>

about DL prevalence and MR imaging characteristics.⁶ Including highly sensitive examinations in the diagnostic workflow may potentially lead to earlier diagnosis and start of treatment⁵ and provide structural correlates for patients' asymptomatic visual loss.⁴ Furthermore, in the monitoring phase, an improved detection of new-onset lesions may help tailor treatment in individual patients.⁷

In a group of patients with MS with and without a history of AON and in a group of healthy controls (HC), we tested whether a dedicated inversion-recovery (STIR)-prepared T2-weighted technique, combining high spatial resolution and tissue contrast characteristics, the "3D-T2-STIR-ZOOMit" (Siemens), may improve DL diagnostic performance in the aVPs with respect to 2D-T2-STIR, the current standard technique.⁸

MATERIALS AND METHODS

The study was authorized by the Ethics Committee of Canton Ticino, Switzerland (2017-00814-CE3224, May 24, 2017). All participants provided written informed consent.

Study Participants

This was a prospective, cross-sectional, single-center study including 49 adult patients with relapsing-remitting MS according to the 2010 McDonald criteria⁹ and with or without previous AON history (pON+ and pON-, respectively), and 24 HC. Participants were enrolled between November 2017 and March 2019 at the MS Center of the Ospedale Regionale di Lugano (Neurocenter of Southern Switzerland), Switzerland, the regional center for neuro-ophthalmologic disorders. AON diagnosis was based on a history of visual acuity and color detection loss, typical field deficits, ocular pain, and fundus examination. MR imaging and visual evoked

potentials (prolonged P100 latency) were used as supportive tools when needed. All participants with MS were relapse- and steroid therapy-free for at least 3 months before enrollment. Specific exclusion criteria were other neurologic and ophthalmologic disorders (glaucoma, ocular hypertension, retinopathy, maculopathy).

MR Imaging Acquisition

Acquisition parameters of 3D-T2-STIR-ZOOMit and 2D-T2-STIR are reported in Table 1.

3D-T2-STIR-ZOOMit. We adapted the vendor-provided default T2-weighted sequence for small-FOV imaging with selective region excitation on a 3T Magnetom Skyra (Siemens) scanner^{10,11} with a 64-channel head/neck coil. We applied a nonselective inversion recovery preparation pulse,^{12,13} using an acquisition voxel size of 0.6 mm³. Scan duration was 8 minutes 54 seconds.

2D-T2-STIR. A standard 2D-T2-STIR sequence, with 2.5-mm section thickness, was acquired on the coronal plane, covering the orbits and the intracranial aVPs. The scan duration was 2 minutes 57 seconds

Additional information about sequences, image acquisition, and preparation, is provided in the Online Supplemental Data.

Image Quality

Figure 1 shows the normal anatomy of the aVPs as depicted by 3D-T2-STIR-ZOOMit and the segment boundaries defined for the analyses: intraorbital (iOrb), intracanalicular (iCanal), and intracranial (iCran) optic nerves, OC, and OT. The corresponding anatomic landmarks were also used for 2D-T2-STIR. One neuroradiologist (A.C.) and 1 neurologist (C.G.) with >15 years of experience in MS imaging rated, in each of the 5 aVP segments, field

inhomogeneity and motion-related artifacts, according to a previously used scale: 0 = no relevant artifacts; 1 = mild artifacts not preventing image analysis; 2 = artifacts preventing accurate image analysis.¹⁴

Image Reading Sessions

Two neuroradiologists (E.P. and L.R.) with >15 years of experience in MS imaging performed 3 reading sessions each, >3 months apart to avoid recall bias.

Session 1. The blinded readers reviewed separately the 3D-T2-STIR-ZOOMit and 2D-T2-STIR image sets in a

Table 1: Acquisition parameters for 3D-T2-STIR-ZOOMit and 2D T2-STIR

Parameter	3D-T2-STIR-ZOOMit	2D-T2-STIR
Mode	3D	2D
Acquisition plane	Transversal	Coronal
TR/TE (ms)	240/119	4880/101
Magnetization preparation	Non-selective STIR	Non-selective STIR
TI (ms)	220	220
FOV read/FOV phase	80 mm × 100%	180 mm × 100%
Base resolution/phase/section	128/100%/100%	320/100%/–
Acquired voxel size (X, Y, Z) (mm)	0.6, 0.6, 0.6	0.6, 0.6, 2.5
Interpolated voxel size (X, Y, Z) (mm)	0.3, 0.3, 0.6	
Flip angle	Variable	140°
Turbo factor	46	35
Averages	1.4	1
Acceleration factor (GRAPPA)	2	None
Scan duration (min/sec)	8/54	2/57

Note:—GRAPPA, generalized autocalibrating partially parallel acquisition; STIR, short tau inversion recovery.

Table 2: Confusion matrix illustrating DL detection rates of 3D-T2-STIR-ZOOMit and 2D-T2-STIR per each aVP segment in all patients with MS^a

		3D-T2-STIR-ZOOMit									
		iOrb–	iOrb+	iCanal–	iCanal+	iCran–	iCran+	OC–	OC+	OT–	OT+
2D-T2-STIR	–	67 (69.8)	9 (9.4)	68 (70.8)	8 (8.3)	87 (90.6)	7 (7.3)	79 (82.3)	16 (16.7)	86 (89.6)	10 (10.4)
	+	0 (0)	20 (20.8)	4 (4.2)	16 (16.7)	0 (0)	2 (2.1)	0 (0)	1 (1.0)	0 (0)	0 (0)

^aData are number of DLs (n=96, for each aVP segment) with percentages in parentheses and refer to 96 observations (left and right sides together in 48 patients) in each aVP segment. Absence of a lesion is indicated with –; presence, with +.

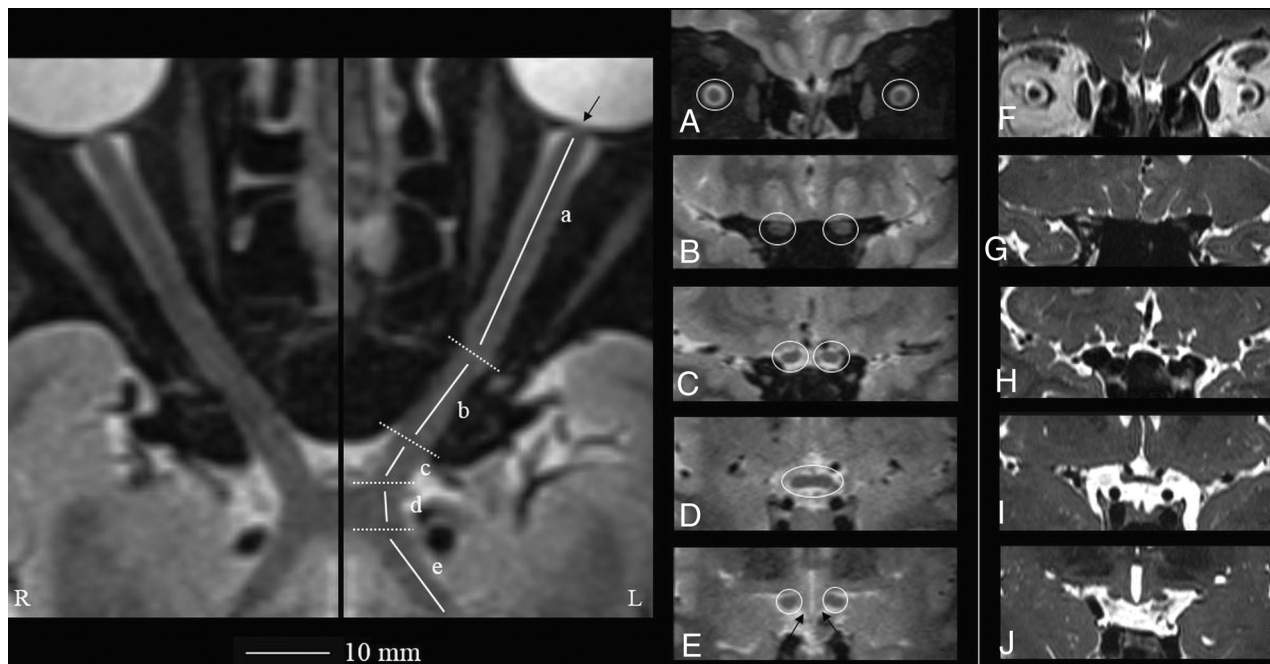


FIG 1. Geometrically unbiased, high-resolution representation of the aVP segment anatomy by 3D-T2-STIR-ZOOMit (healthy control No. 9001). The left panel shows curved reconstructions along the true long axis of the right and left aVPs. The *thin arrow* points to the porus opticus. Coronal-oblique reconstruction images corresponding to the iOrb (A, from the eye bulb to the optic canal), iCanal (B, in the optic canal), and iCran (C, from the optic canal to the chiasm) segments and OC (D) and OT (E) segments highlighted in *white circles* are presented. By comparison, the right panel (F–J, different healthy volunteer) shows corresponding coronal-oblique images obtained with a 3D-ZOOMit standard sequence without the STIR preparation pulse. Note substantial contrast resolution gain with 3D-T2-STIR-ZOOMit, particularly at interfaces between different signal tissues and between the OT and adjacent hypothalamus (*thin arrows* in E).

random order. 3D-T2-STIR-ZOOMit images were presented in orthogonally reconstructed planes, whereas 2D-T2-STIR images were presented in the acquisition (coronal) plane. To assess the presence of a lesion, we used a previously employed binary scale:¹⁴ 0 = no lesion; 1 = lesion. Lesions were defined as areas of signal hyperintensity, referenced to the normal-appearing white matter of the frontal lobes, either partially or completely involving the whole aVP short-axis section. A consensus was reached after resolving discrepancies during a subsequent separate session.

Session 2. To test the hypothesis that 3D-T2-STIR-ZOOMit may detect false-positive lesions in HC assuming that these had no DLs, the readers performed an additional joint session on scans of the 19 HC and 19 randomly chosen participants with MS.

Session 3. To assess scan-rescan reproducibility, a final joint session compared the 3D-T2-STIR-ZOOMit images re-acquired from 12 participants with MS with those from session 1.

Statistical Analysis

Categorical variables were reported with count and percentages; continuous variables, with mean (SD) or median and interquartile range. Interrater reliability was reported with accuracy, Cohen κ , and their 95% CIs. A Cohen κ of >0.8 suggests a strong level of agreement between the raters. To assess scan-rescan reproducibility of 3D-T2-STIR-ZOOMit images, we calculated the interclass correlation coefficient. Between-sequence detection differences and the effects of DL side and location in the aVPs, accounting for within-patient correlation, were assessed using a binomial mixed-

effects logistic model. OR, 95% confidence intervals, and *P* values were reported.

P values $< .05$ were considered significant. R statistical and computing software, Version 3.6.0 (<http://www.r-project.org/>) was used for all analyses.

RESULTS

Participant Characteristics

Of 73 initially included participants (49 with MS, 24 HC), 48 participants with MS (39.1 [SD, 13.1] years of age, 30 women) with ($n = 19$) or without ($n = 29$) past optic neuritis (pON+/pON-) and 19 HC (35.1 [SD, 8.1] years of age, 10 women) were finally evaluated (Fig 2). On image inspection, scans of 1 participant with MS and 3 HC were discarded due to poor image quality in all aVP segments (movement) and also scans of 2 HC for coil-related artifacts (shading artifacts). The main demographic and clinical characteristics of participants with MS are presented in the Online Supplemental Data. Patients' neurologic impairment severity, assessed with the Expanded Disability Status Scale,¹⁵ was mild (median = 2; range, 1–3.5). Twenty-nine participants (60.4%) were pON-. Among those with pON+ ($n = 19$, 39.6%), 4 had bilateral AON. When we counted individual eyes, 73 (76%) had no AON and 23 (24%) had previous AON.

Image Quality

The Online Supplemental Data illustrate samples of the encountered artifacts. As for 3D-T2-STIR-ZOOMit, grade I movement artifacts were noted in all aVP segments in 3 patients with MS

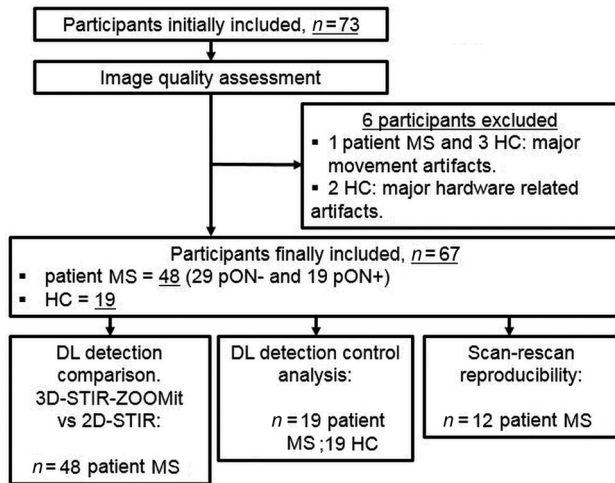


FIG 2. Flow chart showing the numbers of participants and healthy participants with MS included in the study who were assessed and evaluated.

and only in the iOrb segment in 7 patients. Field inhomogeneity artifacts occurred in the iCanal segment in 11 patients with grade 1 and 6 with grade 2, and in 3 (grade 1) and 3 (grade 2) HC. No relevant artifacts were recorded on 2D-T2-STIR images.

3D-T2-STIR-ZOOMit Reliability

Interrater Reliability. Accuracy for 3D-T2-STIR-ZOOMit was 0.96 (95% CI, 0.93–0.97), and the Cohen κ was 0.85 (95% CI, 0.78–0.91), whereas accuracy for 2D-T2-STIR was 0.98 (95% CI, 0.97–0.99) and the Cohen κ was 0.90 (95% CI, 0.83–0.97). The strong level of interrater reliability for 3D-T2-STIR-ZOOMit and the overlapping κ confidence intervals suggest similar agreement between the techniques.

HC Analysis. We assessed 19 HC and 19 randomly chosen participants with MS, for a total of 380 sites (10 aVP segments in 38 participants). At consensus, 28 lesions were found in participants with MS, whereas no lesions were found in HC. Agreement was 0.995 (95% CI, 0.981–0.999). κ was 0.96 (95% CI, 0.91–0.99).

For scan-rescan reproducibility, the ICC was 0.97 (95% CI, 0.96–0.98), $F(120) = 38$, $P < .001$, indicating excellent reproducibility (Online Supplemental Data).¹⁴

DL Detection Comparison: All Participants with MS

Figure 3 illustrates the DL appearance on 3D-T2-STIR-ZOOMit sequences. Lesions involved either completely or, partially, the aVP cross-section. Subtle and diffuse signal abnormalities without definite segmental boundaries were also encountered, but this pattern was not systematically assessed in the present investigation.

Ten aVP segments (5 for each side) were reviewed in 48 participants with MS and 96 eyes, for both techniques. Table 2 presents the DL detection rates of 3D-T2-STIR-ZOOMit and 2D-T2-STIR. With 3D-T2-STIR-ZOOMit, more than twice the DLs ($n = 89$) were detected compared with 2D-T2-STIR ($n = 43$) (OR = 2.7; 95% CI, 1.7–4.1; $P < .001$). Detection capability differences were similar across sides (right versus left, OR = 1.1; 95%

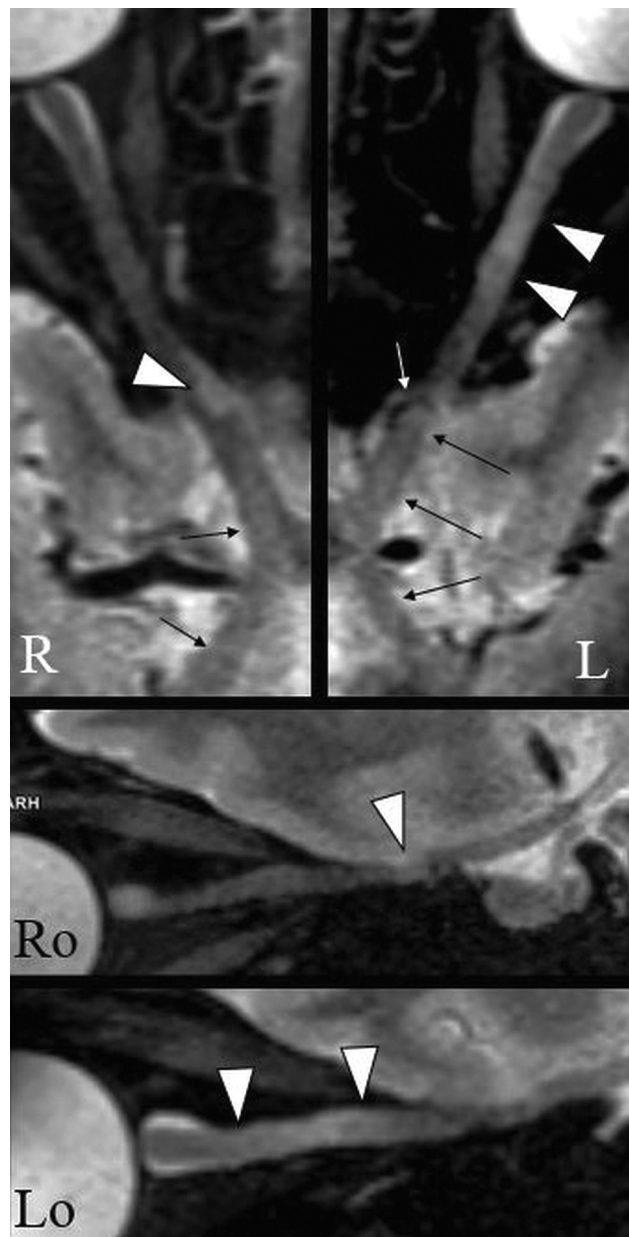


FIG 3. An example of the DL appearance on 3D-T2-STIR-ZOOMit images in a patient with MS (No. 0034). The upper panel shows curved reconstructions along the true long axis of the right and left aVPs. Focal signal hyperintensities indicate DLs with partial (right) and complete (left) involvement of the optic nerve cross-section (arrowheads). There are areas of diffuse signal hyperintensity with no definite boundaries along the aVP (thin arrows), possibly related to diffuse demyelination and/or degeneration. The white arrow indicates the ophthalmic artery causing nerve impression. Ro and Lo images present sagittal-oblique reconstructions of R and L.

CI, 0.7–1.7; $P = .47$), but not across segments ($\chi^2 [df=4] = 20.4$; $P < .001$).

In particular, in the iOrb segment (Fig 4), 9 of 29 DLs (31%, corresponding to 10.1% of all aVP lesions) detected by 3D-T2-STIR-ZOOMit were missed by 2D-T2-STIR.

In the iCanal segment only, 4 DLs were detected with 2D-T2-STIR, but not with 3D-T2-STIR-ZOOMit. Of these, one occurred in a participant with MS with grade 2 movement artifacts, and

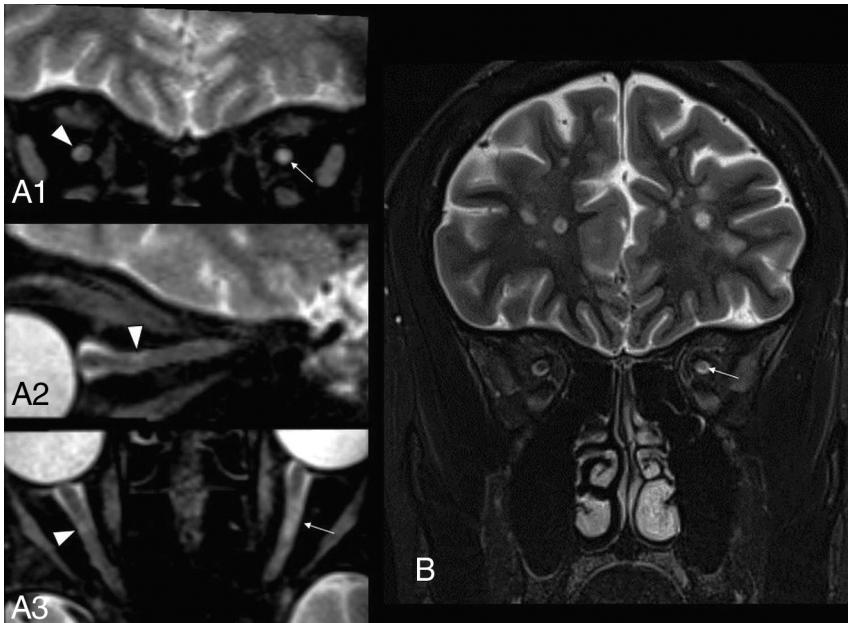


FIG 4. Comparison of extra cranial aVP detection in a participant with MS with previous unilateral AON on the left side (patient with MS No. 0038). A₁₋₃, A very small, asymptomatic DL partially involving the superolateral aspect of the right iOrb segment (arrowheads on coronal, sagittal-oblique, and axial-oblique images) was missed on the 2D-T2-STIR image (B). A larger L iOrb lesion was instead detected by both sequences (thin arrows in A₁, A₃ and B), possibly representing chronic changes related to the previous AON.

one was on a scan with grade 2 magnetic field inhomogeneity artifacts. Two DLs were missed by 3D-T2-STIR-ZOOMit but could be retrospectively noticed after being detected by 2D-T2-STIR.

If one takes all intracranial segments together (iCran, OC, and OT), 33 of 36 DLs (corresponding to 40.5% of all aVP lesions) detected by 3D-T2-STIR-ZOOMit were missed by 2D-T2-STIR. These DLs appeared generally smaller than the extracranial lesions (Fig 5). OT lesions, representing 10.4% of all aVP lesions, were characterized by signal contrast loss between the OT and the adjacent hypothalamus gray matter (Fig 5). Due to a resemblance to lobster antennas, we propose this appearance as the “lobster antenna” sign.

DL Detection Comparison: pON+ and pON-

3D-T2-STIR-ZOOMit revealed ≥ 1 lesion in 18 of the 19 (94.7%) pON+, and in 13 of the 29 (44.8%) pON- patients whereas 2D-T2-STIR revealed lesions only in 17 patients with pON+ (89.5%) and 5 (17.2%) patients with pON- (Online Supplemental Data and Fig 6). DLs were about 6.5 times more frequently found in pON+ than in pON- (OR=6.5; 95% CI, 2.8–15.1; $P < .001$). Lesion-detection probability using 3D-T2-STIR-ZOOMit was 1.8 times higher in pON+ (OR = 1.8; 95% CI, 1.2–3.1; $P = .01$) and 5.9 times higher in pON- (OR = 5.9; 95% CI, 2.5–13.8; $P < .001$) than when using 2D-T2-STIR. The larger detection increment in pON- compared with pON+ was statistically significant (P for interaction = .049). Among the 73 individual eyes with no AON, 3D-T2-STIR-ZOOMit revealed 32 DLs, whereas 2D-T2-STIR revealed only 4.

DISCUSSION

We showed that 3D-T2-STIR-ZOOMit may detect a substantially larger numbers of aVP DLs, particularly in the intracranial segments and in patients without pON-, compared with the standard 2D-T2-STIR.^{5,8} Because optic nerve lesions represent a hallmark of MS disease dissemination,¹⁶ including highly sensitive MR imaging examinations in the diagnostic workflow may lead to earlier diagnosis and start of treatment⁵ and provide structural correlates for patients’ asymptomatic vision loss.⁴ The technique specificity was supported by the absence of false-positive lesions in HC.

The classic 2D-T2-STIR uses a STIR pulse to both suppress orbital fat and increase image contrast by exploiting the T1 relaxation time difference among tissues,^{12,13} ultimately leading to an increased lesion conspicuity with respect to non-inversion recovery-prepared T2-TSE sequences using spectral fat saturation. However, 2D imaging offers suboptimal demarcation of anatomic details¹⁷⁻²⁰ because of through-plane partial volume effects.²¹ The ZOOMit is a recently developed MR imaging technology that focuses on data sampling by applying an excitation pulse that is spatially selective in both section and phase-encoding directions.^{10,11} The dedicated 3D-T2-STIR-ZOOMit technology allowed disclosing aVP disease dissemination with a 5.9-fold probability increase compared with 2D-T2-STIR, thus revealing a substantially larger number of clinically asymptomatic DLs.

3D-T2-STIR-ZOOMit detected at least 1 DL in 44.8% of patients with pON-. Using a 3D double inversion recovery sequence, Sartoretti et al²² identified lesions in 72% of a group of patients with MS without visual symptoms within the past 3 years. Patient selection criteria might, at least in part, account for such a relatively higher percentage because patients who had visual symptoms before the previous 3 years might have been included. Indeed, with the same technique, Hadhoum et al²³ found lesions in 38.5% of optic nerves without AON history, while Riederer et al²⁴ observed subclinical lesions in 18% of their patients. However, these studies did not assess the OT, whose lesion burden constituted 10.4% of all DLs in our participants with MS.

Most interesting, DLs frequently targeted the intracranial aVP segments, which, altogether, had 40.5% of aVP lesions, a figure that was largely missed with 2D-T2-STIR. Although brain 3D techniques used in clinical practice, such as double inversion recovery or FLAIR, might detect a relatively higher number of intracranial aVP lesions than 2D-STIR, their spatial resolution is substantially lower than that of 3D-T2-STIR-ZOOMit.^{14,25} Here, we were able to disclose a frequent occurrence of the OT involvement in MS,

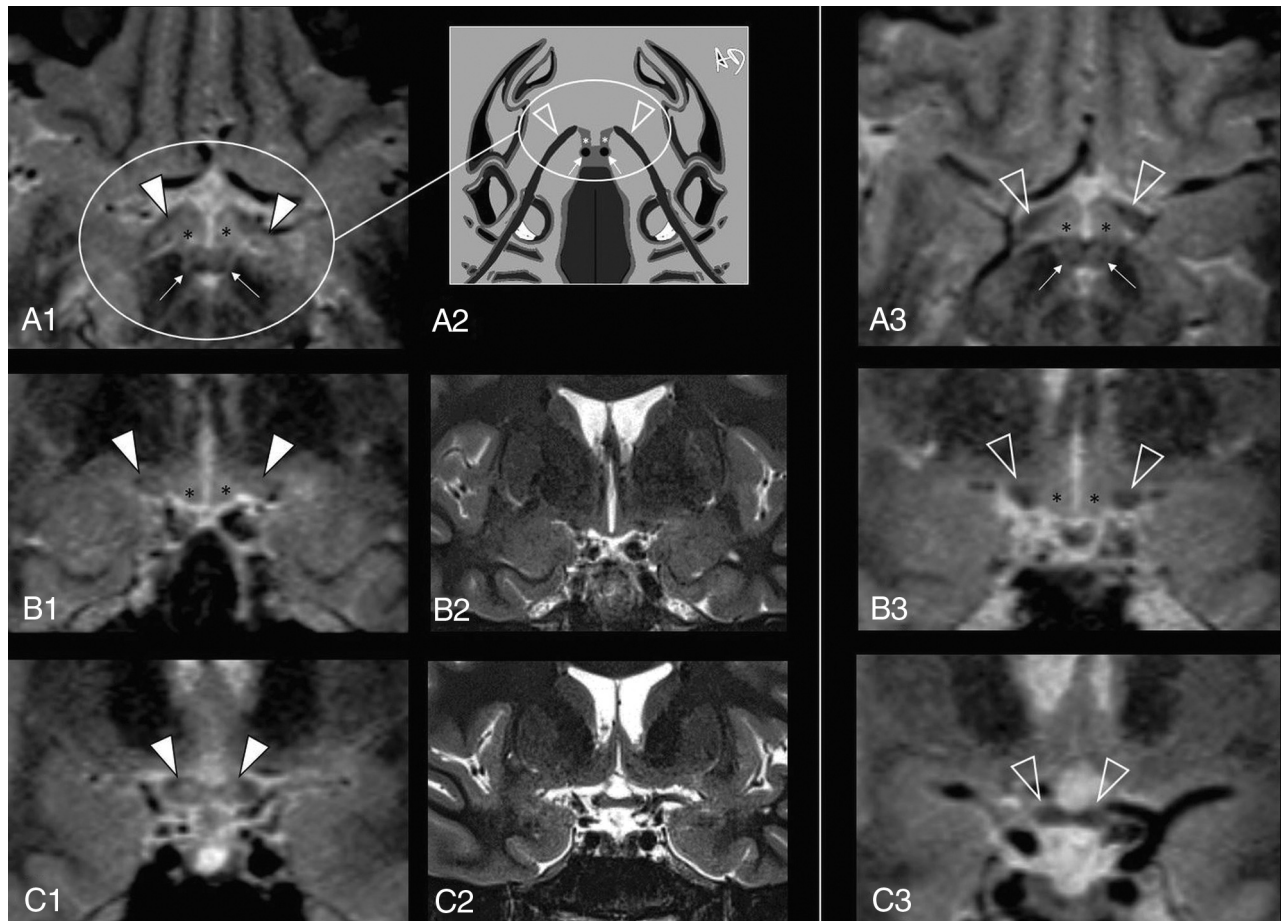


FIG 5. Intracranial aVP detection of asymptomatic DL in a participant with MS without a previous AON history (patient with MS No. 0020) on 3D-T2-STIR-ZOOMit images. A₁, and B₁, Bilateral DLs partially affecting the OTs and impairing tissue contrast (*arrowheads*) with the adjacent hypothalamus ventrolateral aspects (*asterisks*). C₁, Further depiction of DLs with partial involvement of the OC (*arrowheads*). All these lesions were not detectable on 2D-T2-STIR (*middle panel, B₂, C₂*). The *right panel (A₃, B₃, C₃)* provides the reference normal anatomy (*empty arrowheads*) from a healthy control (No. 9005). Because of the axial plane appearance of the OTs and hypothalamus ventrolateral aspects resembling lobster antennas, we propose the “lobster antenna” sign to indicate loss of normal tissue contrast between the OT and hypothalamus. *Thin arrows* in A₁ and A₃ indicate the mammillary bodies, corresponding to the lobster’s eyes in the artwork (A₂). Courtesy of Dr. Andrea Diociai.

leading to the proposed lobster antenna sign appearance. Future investigations in larger cohorts and longitudinal studies are warranted to compare with other autoimmune disorders typically involving this region, such as the neuromyelitis optica spectrum and the antimyelin oligodendrocyte glycoprotein antibodies disorders.² Indeed, a detailed knowledge of DL appearance and spatial distribution patterns in the entire aVP may support prompt differential diagnosis and appropriate treatment initiation.

Our technique has several limitations. First, we did not use post-mortem specimens as a criterion standard to definitely assess 3D-T2-STIR-ZOOMit accuracy. As far as we are aware, no previous radiologic-pathologic correlation data are available in the literature for the aVP. However, our control analysis showed that 3D-T2-STIR-ZOOMit was unlikely to provide false-positive results in healthy participants. Moreover, between-reader agreement and scan-rescan consistency were high, suggesting adequate technique reproducibility. Second, scan duration was relatively long, and images from 3 participants had to be discarded for severe movement artifacts. Implementation in the clinical setting requires appropriate hardware as well as patient coaching before the examination (see

the MATERIALS AND METHODS section). This study was performed in patients with relatively mild disability. Future sequence developments, using, for example, compressed sensing,²⁶ 3D parallel imaging acceleration techniques,²⁷ and/or motion-correction techniques²⁸ may facilitate image acquisition by reducing the scan time and movement artifacts, therefore optimizing the examination workflow. Third, field inhomogeneity artifacts preventing visualization of the iCanal segment were relatively frequent, leading to a reduced DL-detection capability at this level. Finally, we did not assess here whether the increased sensitivity allowed by 3D-T2-STIR-ZOOMit may help to explain patients’ subclinical vision loss and to predict disability accrual and clinical relapses. Future studies are planned to investigate the relationships among DL load, precise ophthalmologic measurements of visual acuity loss, and neurologic disability.

CONCLUSIONS

We showed that the assessment of MS disease dissemination in the aVP may be substantially improved using dedicated high-spatial-resolution and contrast-optimized 3D-T2-STIR-ZOOMit

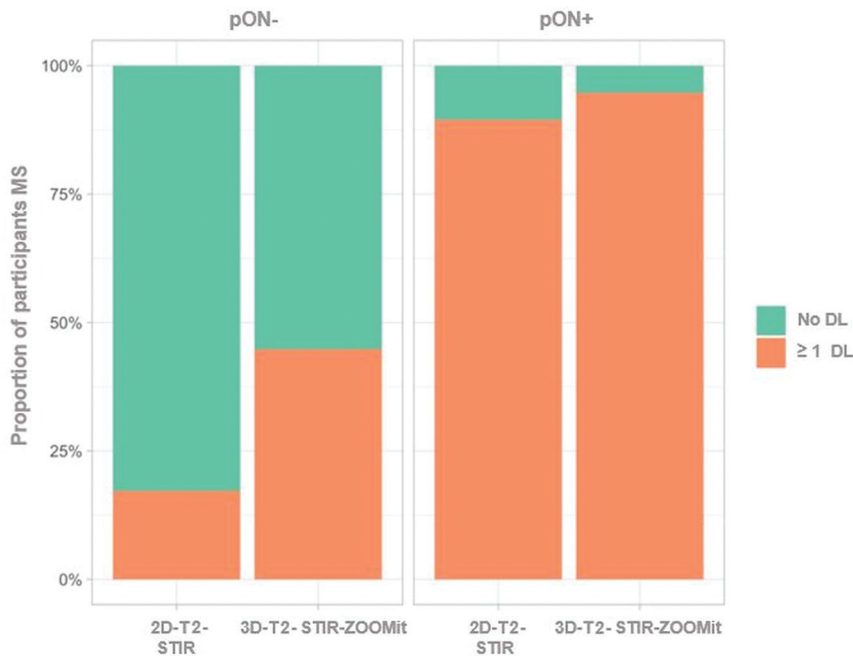


FIG 6. Proportion of participants with MS with at least 1 identified DL (at any site and any side) by previous AON history (pON-/pON+) and MR imaging technique (2D-T2-STIR/3D-T2-STIR-ZOOMit).

images. Advantages are particularly beneficial at the level of the intracranial segments and in patients without a history of acute optic neuritis.

ACKNOWLEDGMENTS

The authors thank Liliane Petrini, Neurocenter of Southern Switzerland (Lugano, Switzerland), for help with the bibliography and for finalizing the manuscript; Dr Andrea Diociai, University of Genoa (Italy), for Fig 5 artwork; and Mr. Navarajah Nadarajah, Ospedale Regionale di Lugano (Lugano, Switzerland), for MR imaging data acquisition.

Disclosures: Emanuele Pravata—RELATED: Grant: Scientific Research Advisory Board of the Ente Ospedaliero Cantonale, Swiss Multiple Sclerosis Society*; UNRELATED: Grants/Grants Pending: Velux Stiftung.* Maria Pia Sormani—UNRELATED: Board Membership: Biogen, Merck, Sanofi, Roche, Novartis, Immunic; Consultancy: Biogen, Merck, Sanofi, Roche, Novartis, Immunic, Celgene; Grants/Grants Pending: Roche, Merck; Payment for Lectures Including Service on Speakers Bureaus: Biogen, Merck, Sanofi, Roche, Novartis, Immunic, Celgene. Rosaria Sacco—UNRELATED: Board Membership: Employer, Department of Neurology, Regional Hospital Lugano, Lugano, Switzerland receives financial support from AbbVie, Almirall, Biogen Idec, Celgene, Sanofi, Merck, Novartis, Teva Pharmaceuticals, Roche*; Payment for Lectures Including Service on Speakers Bureaus: Novartis, Celgene; Payment for Development of Educational Presentations: Sanofi; Travel/Accommodations/Meeting Expenses Unrelated to Activities Listed: Merk. Alain Kaelin-Lang—UNRELATED: Consultancy: Advisory board about the therapeutic use of Abobotulinum toxinA to treat spasticity, Ipsen*; Employment: Ente Ospedaliero Cantonale, Bellinzona, Switzerland; Grants/Grants Pending: unrestricted research grant, Merz Pharma*; Travel/Accommodations/Meeting Expenses Unrelated to Activities Listed: Movement Disorders Meeting, Nizza, 2019; Honk-Kong, 2018; companies: Allergan, Merz Pharma.* Chiara Zecca—UNRELATED: Consultancy: Biogen, Celgene, Lilly, Merck, Sanofi, Teva Pharmaceuticals, Roche*; Grants/Grants Pending: Biogen, Merck*; Payment for Lectures Including Service on Speakers Bureaus: Novartis, Celgene, Lilly, Novartis, Teva Pharmaceuticals.* Claudio Gobbi—RELATED: Grants: Scientific Research Advisory Board of the Ente Ospedaliero Cantonale, Swiss Multiple Sclerosis Society, Comments: Scientific Research Advisory Board of the Ente

Ospedaliero Cantonale*; UNRELATED: Board Membership: Biogen Idec, Celgene, Sanofi, Merck Serono, Novartis, Roche, and Teva Pharmaceuticals*; Consultancy: Biogen Idec, Celgene, Sanofi, Merck Serono, Novartis, Roche, and Teva Pharmaceuticals*; Grants/Grants Pending: Biogen Idec, Celgene, Sanofi, Merck Serono, Novartis, Roche, and Teva Pharmaceuticals, * *Money paid to the institution.

REFERENCES

1. Reich DS, Lucchinetti CF, Calabresi PA. **Multiple sclerosis.** *N Engl J Med* 2018;378:169–80 [CrossRef Medline](#)
2. Dutra BG, Da Rocha AJ, Nunes RH, et al. **Neuromyelitis optica spectrum disorders: spectrum of MR imaging findings and their differential diagnosis.** *Radiographics* 2018;38:169–93 [CrossRef Medline](#)
3. Ulrich J, Groebke-Lorenz W. **The optic nerve in multiple sclerosis: a morphological study with retrospective clinico-pathological correlations.** *Neuro-Ophthalmology* 1983;3:149–59 [CrossRef](#)
4. Balcer LJ, Frohman EM. **Evaluating loss of visual function in multiple sclerosis as measured by low-contrast letter acuity.** *Neurology* 2010;74:S16–23 [CrossRef Medline](#)
5. Filippi M, Rocca MA, Ciccarelli O, et al. **MRI criteria for the diagnosis of multiple sclerosis: MAGNIMS consensus guidelines.** *Lancet Neurol* 2016;15:292–303 [CrossRef Medline](#)
6. Thompson AJ, Banwell BL, Barkhof F, et al. **Diagnosis of multiple sclerosis: 2017 revisions of the McDonald criteria.** *Lancet Neurol* 2018;17:162–73 [CrossRef Medline](#)
7. Sormani MP, De Stefano N. **Defining and scoring response to IFN- β in multiple sclerosis.** *Nat Rev Neurol* 2013;9:504–12 [CrossRef Medline](#)
8. Petzold A, Wattjes MP, Costello F, et al. **The investigation of acute optic neuritis: a review and proposed protocol.** *Nat Rev Neurol* 2014;10:447–58 [CrossRef Medline](#)
9. Polman CH, Reingold SC, Banwell B, et al. **Diagnostic criteria for multiple sclerosis: 2010 Revisions to the McDonald Criteria.** *Ann Neurol* 2011;69:292–302 [CrossRef Medline](#)
10. Blasche M, Riffel P, Lichy M. **TimTX TrueShape and syngo ZOOMit: technical and practical aspects.** *MAGNETOM Flash* 2012 https://cdn0.scrvt.com/39b415fb07de4d9656c7b516d8e2d907/1800000000118051/a06d5db36c83/TimTX_TrueShape_and_syngo_Zoomit_Aspects_1800000000118051.pdf. Accessed January 01, 2020
11. Fang S, Bai HX, Fan X, et al. **A novel sequence: ZOOMit-blood oxygen level-dependent for motor-cortex localization.** *Clin Neurosurg* 2020;86:E124–32 [CrossRef Medline](#)
12. Bot JC, Barkhof F, Lycklama À, et al. **Comparison of a conventional cardiac-triggered dual spin-echo and a fast STIR sequence in detection of spinal cord lesion in multiples sclerosis.** *Eur Radiol* 2000;10:753–58 [CrossRef Medline](#)
13. Thorpe JW, MacManus DG, Kendall BE, et al. **Short tau inversion recovery fast spin-echo (fast STIR) imaging of the spinal cord in multiple sclerosis.** *Magn Reson Imaging* 1994;12:983–89 [CrossRef Medline](#)
14. Hodel J, Outteryck O, Bocher AL, et al. **Comparison of 3D double inversion recovery and 2D STIR FLAIR MR sequences for the imaging of optic neuritis: pilot study.** *Eur Radiol* 2014;24:3069–75 [CrossRef](#)

15. Kurtzke JF. **Rating neurologic impairment in multiple sclerosis: An Expanded Disability Status Scale (EDSS).** *Neurology* 1983;33:1444–52 [CrossRef Medline](#)
16. Geraldes R, Ciccarelli O, Barkhof F, et al. MAGNIMS study group. **The current role of MRI in differentiating multiple sclerosis from its imaging mimics.** *Nat Rev Neurol* 2018;14:199–213 [CrossRef Medline](#)
17. Bink A, Schmitt M, Gaa J, et al. **Detection of lesions in multiple sclerosis by 2D FLAIR and single-slab 3D FLAIR sequences at 3.0 T: initial results.** *Eur Radiol* 2006;16:1104–10 [CrossRef Medline](#)
18. Molyneux PD, Tubridy N, Parker GJ, et al. **The effect of section thickness on MR lesion detection and quantification in multiple sclerosis.** *AJNR Am J Neuroradiol* 1998;19:1715–20 [Medline](#)
19. Moraal B, Roosendaal SD, Pouwels PJ, et al. **Multi-contrast, isotropic, single-slab 3D MR imaging in multiple sclerosis.** *Eur Radiol* 2008;18:2311–20 [CrossRef Medline](#)
20. Kallmes DF, Hui FK, Mugler JP. **Suppression of cerebrospinal fluid and blood flow artifacts in FLAIR MR imaging with a single-slab three-dimensional pulse sequence: Initial experience.** *Radiology* 2001;221:251–55 [CrossRef Medline](#)
21. Kneeland JB, Shimakawa A, Wehrli FW. **Effect of intersection spacing on MR image contrast and study time.** *Radiology* 1986;158:819–22 [CrossRef Medline](#)
22. Sartoretti T, Sartoretti E, Rauch S, et al. **How common is signal-intensity increase in optic nerve segments on 3D double inversion recovery sequences in visually asymptomatic patients with multiple sclerosis?** *AJNR Am J Neuroradiol* 2017;38:1748–53 [CrossRef Medline](#)
23. Hadhoum N, Hodel J, Defoort-Dhellemmes S, et al. **Length of optic nerve double inversion recovery hypersignal is associated with retinal axonal loss.** *Mult Scler* 2016;22:649–58 [CrossRef Medline](#)
24. Riederer I, Mühlau M, Hoshi MM, et al. **Detecting optic nerve lesions in clinically isolated syndrome and multiple sclerosis: double-inversion recovery magnetic resonance imaging in comparison with visually evoked potentials.** *J Neurol* 2019;266:148–56 [CrossRef Medline](#)
25. Traboulsee A, Simon JH, Stone L, et al. **Revised recommendations of the consortium of MS centers task force for a standardized MRI protocol and clinical guidelines for the diagnosis and follow-up of multiple sclerosis.** *AJNR Am J Neuroradiol* 2016;37:394–401 [CrossRef Medline](#)
26. Yuhasz M, Hoch MJ, Hagiwara M, et al. **Accelerated internal auditory canal screening magnetic resonance imaging protocol with compressed sensing 3-dimensional T2-weighted sequence.** *Invest Radiol* 2018;53:742–47 [CrossRef Medline](#)
27. Fritz J, Fritz B, Thawait GG, et al. **Three-dimensional CAIPIRINHA SPACE TSE for 5-minute high-resolution MRI of the knee.** *Invest Radiol* 2016;51:609–17 [CrossRef Medline](#)
28. White N, Roddey C, Shankaranarayanan A, et al. **PROMO: real-time prospective motion correction in MRI using image-based tracking.** *Magn Reson Med* 2010;63:91–105 [CrossRef Medline](#)